NSERC-CMIC FOOTPRINTS

Byrne K, Lesage G, Gleeson SA, Lee RG, 2016, Large-scale sodic-calcic alteration around porphyry Cu systems: examples from the Highland Valley Copper district, Guichon batholith, south-central British Columbia, Report, Geoscience BC, 10 p.

NSERC-CMIC Mineral Exploration Footprints Project Contribution 115.

canadamining innovationcouncil

NSERC CRSNG

Large-Scale Sodic-Calcic Alteration Around Porphyry Copper Systems: Examples from the Highland Valley Copper District, Guichon Batholith, South-Central British Columbia

K. Byrne, University of Alberta, Edmonton, AB, kbyrne@ualberta.ca

G. Lesage, Mineral Deposit Research Unit, The University of British Columbia, Vancouver, BC

S.A. Gleeson, Helmholtz Centre Potsdam GFZ German Research Centre for Geosciences, Potsdam, Germany

R.G. Lee, Mineral Deposit Research Unit, The University of British Columbia, Vancouver, BC

Byrne, K., Lesage, G, Gleeson, S.A. and Lee, R.G. (2017): Large-scale sodic-calcic alteration around porphyry copper systems: examples from the Highland Valley Copper district, Guichon batholith, south-central British Columbia; *in* Geoscience BC Summary of Activities 2016, Geoscience BC, Report 2017-1, p. 213–222.

Introduction

Porphyry Cu deposits are the primary source of Cu globally and, although demand ebbs and flows and recycling is increasing, a pipeline of quality projects and resources is needed to replace decreasing inventories (Seedorff et al., 2005; Sillitoe, 2010; Thompson, 2016). Exploration costs and expenditures have increased approximately threefold during the last 12 years (Wilburn et al., 2015; Wood, 2016), yet discovery rates are down and very few new deposits have been found (Sillitoe, 2013). As a result, exploration is moving into underexplored, high-risk political jurisdictions and beneath cover (systems with no surface expression) in known productive belts, necessitating more effective and efficient exploration methodologies and techniques (Sillitoe, 2013; Schodde, 2014; Wood, 2016).

The volume of hydrothermally altered rocks outboard of economically significant concentrations of Cu-Fe–sulphide minerals is termed the porphyry footprint. An understanding of the fluid types that can be present during porphyry Cu formation, how they manifest in the footprint and their spatial distribution with respect to Cu-mineralized portions of the system is critical to developing better exploration tools. This work is part of the Porphyry Copper Footprints Subproject of the Canada Mining Innovation Council (CMIC) and Natural Sciences and Engineering Research Council of Canada (NSERC). Its purpose is to investigate the petrophysical, structural, mineralogical, geochemical and isotopic footprints of the porphyry Cu (±Mo) deposits in the Highland Valley Copper (HVC) district of south-central British Columbia (BC; Figure 1). The Teck Highland Valley Copper Partnership (‘Highland Valley Copper’) is wholly owned and operated by Teck Resources Limited. The district contains proven and probable reserves of

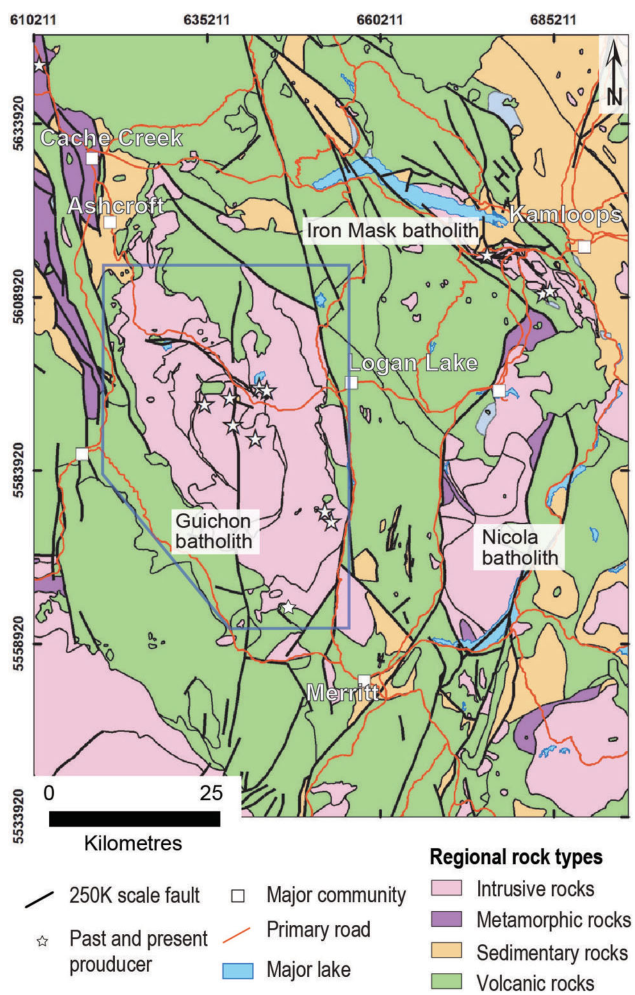

Figure 1. Simplified geology of the Quesnel terrane in southern British Columbia. Geological data from Massey et al. (2005). Blue outline indicates the area shown in Figure 2a.

Keywords: *British Columbia, Guichon batholith, Highland Valley Copper, actinolite, albite, alteration, epidote, Na-Ca, nonmagmatic, porphyry Cu, seawater, sodic-calcic*

This publication is also available, free of charge, as colour digital files in Adobe Acrobat® PDF format from the Geoscience BC website: http://www.geosciencebc.com/s/DataReleases.asp.

577 200 tonnes at 0.29% Cu and 0.007% Mo (Teck Resources Limited, 2016).

Four major porphyry Cu (±Mo) systems, hosted in various intrusive facies of the Late Triassic Guichon batholith, occur in the HVC district (Figure 2a). Exposure and airborne magnetic data indicate that the batholith has an oval shape, elongate to the northwest, with a long axis of approximately 60 km and a short axis of 25 km. Due to its size and low degree of exposure (~3%), the HVC district is a realistic natural laboratory in which to investigate the large-scale footprint of porphyry Cu deposits, integrate disparate geological and geochemical datasets, and develop new methodologies and genetic understanding to aid modern exploration geoscientists.

Two field seasons of mapping and sample collection have been completed. Whole-rock lithogeochemistry, representative rock slabs and thin sections have been processed and analyzed for mineralogy and paragenesis. McMillan (1976, 1985) described argillic and propylitic alteration at HVC; however, the district-scale footprint of sodic-calcic (Na-Ca) alteration had not been recognized in the Guichon batholith before the current study (Figure 2b). This paper presents a description of the Na-Ca alteration in the Guichon batholith and outlines the research question concerning its genesis.

Geological Setting

Regional Geology

The Quesnel terrane in the Canadian Cordillera is characterized by Mesozoic island-arc assemblages comprising volcanic and sedimentary rocks and associated intrusions. The most important rocks for this study are the Late Triassic Nicola Group and the Guichon batholith (Coney et al., 1980; Logan and Mihalynuk, 2014). The Nicola Group consists primarily of andesitic submarine volcanic and associated volcano-sedimentary rocks of island-arc affinity (Preto, 1979; Mortimer, 1987; Ray et al., 1996) that were deposited in a rifted marine basin above an east-dipping subduction zone (Colpron et al., 2007). The I-type, low-K tholeiitic to medium-K calcalkalic Guichon batholith (Figures 1, 2a; Northcote, 1969; McMillan, 1976; D'Angelo, 2016) intruded the ca. 238–202 Ma Nicola Group between ca. 211 and 204 Ma, prior to docking with ancestral North America (Logan and Mihalynuk, 2014; Mihalynuk et al., 2016). The region subsequently underwent Cretaceous shortening and localized Paleogene–Neogene extensional deformation (Colpron et al., 2007).

District Geology

Several texturally and compositionally distinct intrusive facies are recognized in the Guichon batholith (Northcote, 1969; McMillan, 1976; D'Angelo, 2016.). Older marginal and equigranular mafic rocks transition to younger, centrally located, inequigranular to porphyritic felsic facies (Figure 2a). A cluster of at least four porphyry Cu deposits, hosted by the inner intrusive facies, and ~160 additional Cu showings occur in the HVC district (Figure 2a; McMillan et al., 2009; Byrne et al., 2013). Two main stages of mineralization are recognized at HVC (McMillan, 1985; Byrne et al., 2013), and these are separated by ~1 m.y. and intrusion and crystallization of the most evolved intrusive rocks (D'Angelo, 2016). A postmineral, north-trending, dextral strike-slip fault cuts the Valley and Lornex deposits (Figure 2a). Restoring approximately 3.5 km of dextral movement suggests that the Valley and Lornex deposits were once a single porphyry centre (Hollister et al., 1976; McMillan, 1976).

Several features indicate that some of the porphyry centres at HVC were deeply emplaced. Plutonic hostrocks, hornblende bathymetry (D'Angelo, 2016), presence of unidirectional solidification textures and coarse muscovite–dominated (Byrne et al., 2013) early halo-type (or greisen-like) veins imply that the Valley-Lornex cupola and porphyry Cu system was likely emplaced between 4 and 5 km deep (Seedorff et al., 2008; Proffett, 2009; Riedell and Proffett, 2014). A 4–5 km emplacement depth for the Valley-Lornex porphyry system (Figure 3) is also consistent with stratigraphic-thickness estimates for southern Quesnel Nicola Group rocks of between 3 and 6 km (Preto, 1979). At depths greater than approximately 4 km, a single-phase supercritical fluid (of moderate salinity, ~10%) would likely have been stable, possibly leading to mineralization styles and an alteration footprint that are atypical of porphyry environments (Rusk et al., 2008; Richards, 2011b; D'Angelo, 2016). The exposure and prevalence of Na-Ca alteration indicates a deep level of erosion (Figure 3; Seedorff et al., 2008; Halley et al., 2015).

Sodic-Calcic Footprint and Characteristics

Field mapping of domains of high vein density (>0.5 cm/m) highlights fluid pathways within the district (Figure 2b). The Na-Ca facies in the Guichon batholith consists primarily of light green epidote veins with haloes of albite ± fine-grained white mica ± epidote ± chlorite ± actinolite (Figures 4, 5). A key characteristic of the Na-Ca facies is the selective replacement of primary K-feldspar by secondary albite ± fine-grained white mica. Within Na-Ca haloes, primary mafic minerals are replaced by chlorite and localized actinolite, with accessory titanite (Figure 5g). Sodic-calcic veins and haloes occur in ~0.5–2 km wide, north-northeast- and northwest-trending domains that extend along trend from Cu centres for up to 7 km in a nonconcentric pattern (Figure 2b). At the Bethlehem porphyry centre, Na-Ca alteration is most common at depth beneath biotite-altered and Cu-mineralized breccias but is exposed at higher elevations in structurally controlled domains in the

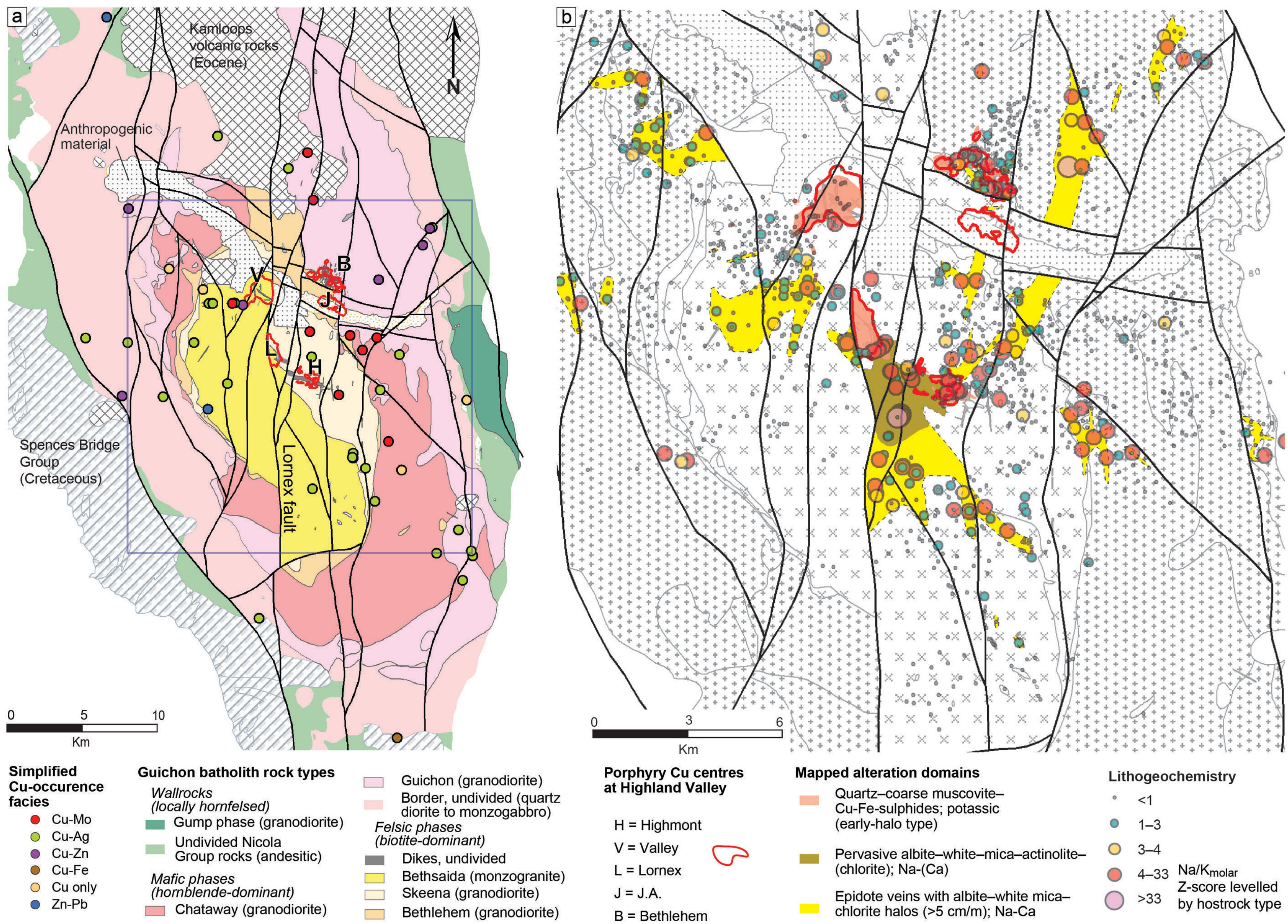

Figure 2. a) Geology of the Guichon batholith (modified after McMillan et al. [2009], Teck Resources Limited and Canada Mining Innovation Council work in the district); also shown are a simplified Cu-occurrence facies interpretation based on compilation of public-domain BC assessment-report data; the blue frame indicates the area shown in Figure 2b. **b)** Distribution of Na-Ca alteration facies in the Guichon district, based on mapped vein and alteration-halo density of greater than ~5 cm/m; the '+' pattern indicates mafic rocks, whereas the coarse 'X' pattern indicates the more felsic rocks in the district.

west and south pit walls. Some isolated domains of Na-Ca facies occur in mafic Border facies rocks. Individual vein orientations are similar to the trend of the larger alteration domains. Outcropping Na-Ca–altered rocks are typically white and fractured, and contrast with surrounding wallrock (Figures 4a, b). Isolated veinlets with narrow haloes, however, are less conspicuous (Figure 4c). Epidote veins typically have an irregular morphology and diffuse walls, and can vary in thickness along strike and down dip (Figures 4c, d). In all examples, K-feldspar is altered to albite within the alteration halo (e.g., Figures 5a–d), whereas plagioclase appears to be less susceptible and only albitized within intense alteration haloes (Figure 5e). Alteration haloes typically range in width between 0.5 and 2 cm but can be up to 1 m wide on large veins. More pervasive albite alteration, locally accompanied by actinolite and relict garnet (mostly retrograded to pumpellyite and chlorite) formed close (150–1000 m) to the porphyry-Cu centres and stocks (Figures 2b, 4b). In hand sample, albite haloes are opaque and the primary twinning and lamellae in igneous feldspars are absent. In thin section, albite-altered feldspar is turbid and associated with coeval, disseminated, fine-grained (~5–10 ì m) white mica and microporosity (Figures 5f, g).

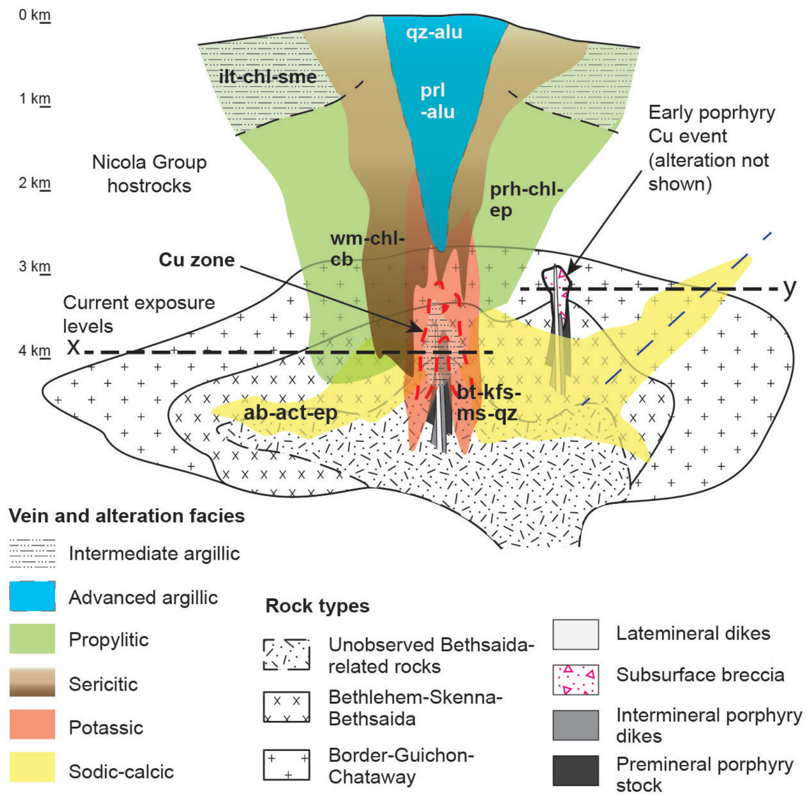

Figure 3. Schematic alteration zonation through the Valley-Lornex porphyry Cu centre hosted in the Guichon batholith (modified after Halley et al., 2015). Note 1) the structural control on Na-Ca–alteration facies; 2) the interpreted emplacement depths and exposure levels of the Valley-Lornex centre (labelled ‘x’) and the shallower Bethlehem breccia–hosted porphyry centre (labelled ‘y’); and 3) the exclusion of the alteration at Bethlehem for clarity. Mineral abbreviations: ab, albite; act, actinolite; alu, alunite; bt, biotite; cb, carbonate mineral; chl, chlorite; ep, epidote; ilt, ilmenite; kfs, K-feldspar; ms, muscovite (coarse grained); prh, prehnite; prl, pyrophyllite; qz, quartz; sme, smectite; wm, white mica–sericite (fine grained).

Prehnite veinlets (±epidote) with plagioclase-destructive white mica–prehnite haloes (±chlorite-vermiculite in hornblende and biotite) constitute the most abundant and widespread alteration facies in the Guichon batholith. The K-feldspar is generally stable within prehnite-vein alteration haloes (Figures 5c, d). Initial shortwave-infrared spectral analysis (TerraSpec 4) of this facies identified a mixed spectrum of white mica (illite), prehnite and subordinate chlorite. Hyperspectral analysis of rock slabs, completed by P. Lypaczewski (CMIC Ph.D. student, University of Alberta), more clearly showed prehnite morphology (vein-fill and disseminated grains in the halo) in rock slabs, and its distribution in the HVC district. Prehnite in rock slabs varies from opaque to light mint-green or dark green and the mineral is susceptible to amaranth stain after etching with HF (Figure 5d). In hand sample, plagioclase altered to white mica is typically pale mint-green in colour. In thin section, small grains (20–100 ì m) of prehnite and more abundant fine-grained clusters (5–20 ì m) of white mica occur together in altered plagioclase crystals. Prehnite veins exhibit a wide range of orientations throughout the batholith. Prehnite veinlets and their associated white mica–chlorite alteration commonly refracture and overprint earlier-formed veins and haloes, resulting in complex alteration patterns in hand sample.

Paragenetic Sequence

Most of the Na-Ca alteration appears to have occurred between the main stages of Cu introduction in the HVC district (Figure 6). Sodic-calcic alteration overprinted biotite–K-feldspar–bornite–chalcocite veins and alteration, and magmatic-hydrothermal breccia, in the Bethlehem system (Figure 4e; Byrne et al., 2013). Narrow (0.2–1 cm) K-feldspar fracture haloes, with and without trace chalcopyrite patina, are found up to 4 km away from the Valley-Lornex and Highmont Cu centres (Lesage et al., 2016). These early-mineral K-feldspar fracture haloes were overprinted by Na-Ca veins at most locations. Locally within the Highmont porphyry Cu centre, however, quartz–chalcopyrite–K-feldspar veinlets appear to crosscut epidote veins with albite haloes (Figures 5a, b). Main-stage veins containing quartz, coarse muscovite and Cu-Fe–sulphide crosscut epi-

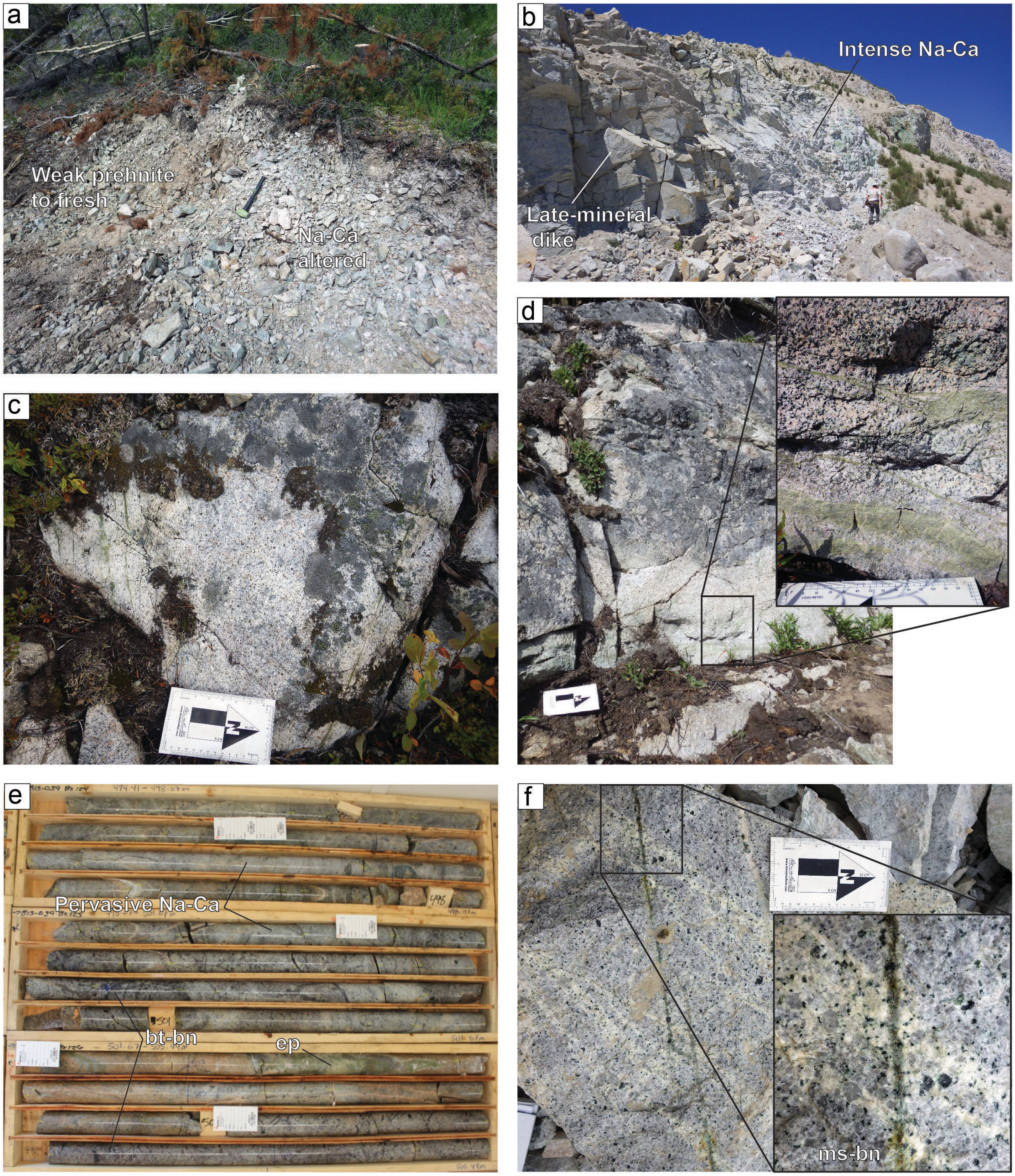

Figure 4. a) Fresh roadcut exposure of Na-Ca alteration in the northeastern part of the batholith. **b)** Intense albite–white-mica alteration above the Bethlehem pit; note the highly fractured Na-altered domain compared to the blocky fracture pattern of a late-mineral dike on the left side of the image. **c)** and **d)** Examples of epidote veins with albite haloes hosted in Guichon granodiorite. **e)** Drillcore from the centre of the Jersey (Bethlehem) porphyry system, showing biotite veins and alteration, and Cu mineralization overprinted by intense albite and epidote-albite (hematite stained); the Na-Ca facies is Cu-grade destructive and leaches Fe. **f)** Premineral quartz and feldspar porphyry stock at Highmont crosscut by albite-fracture haloes (white coloured), which are in turn cut by coarse muscovite-bornite veins. Mineral abbreviations: bn, bornite; bt, biotite; ep, epidote.

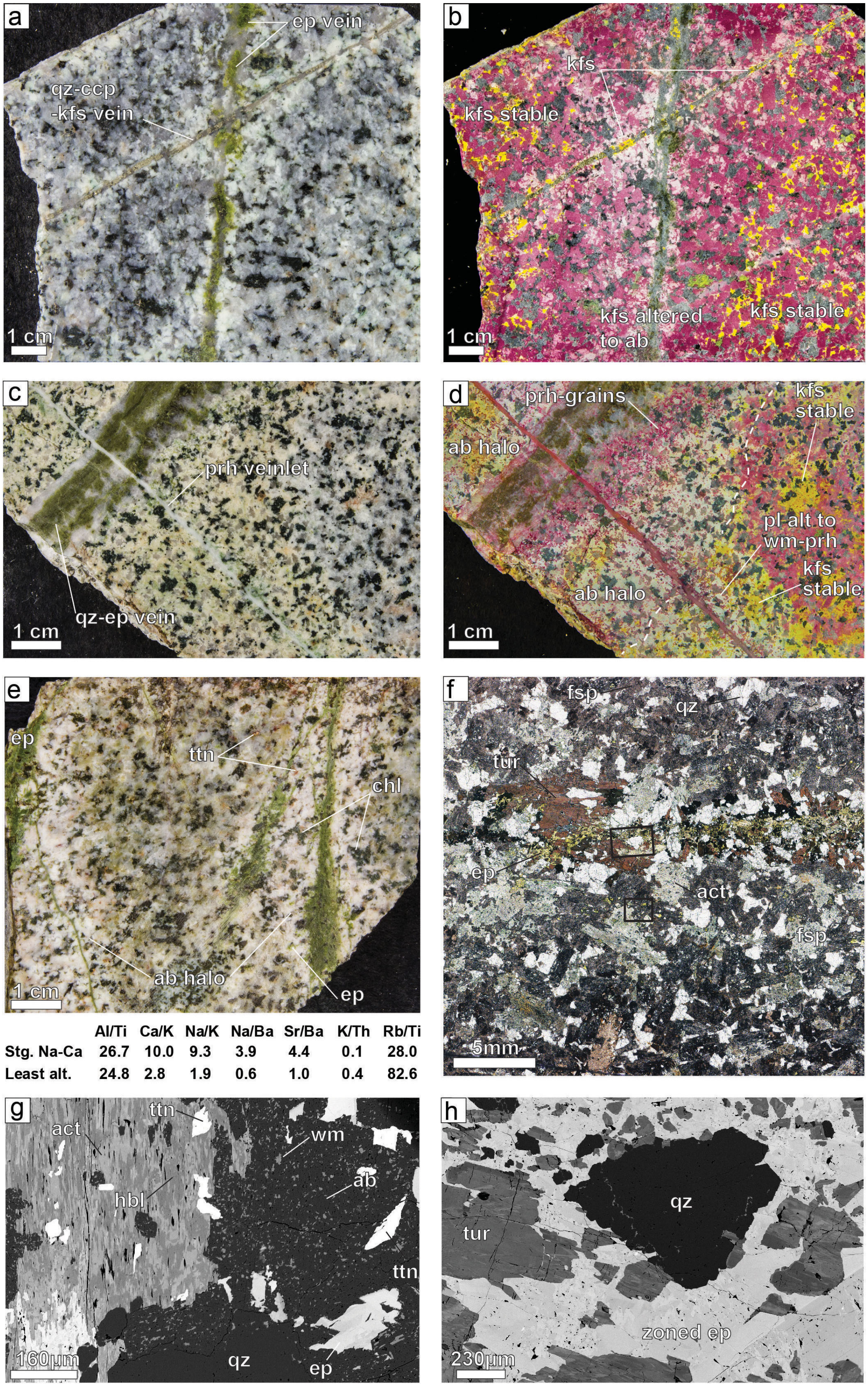

	Al/Ti	Ca/K	Na/K	Na/Ba	Sr/Ba	K/Th	Rb/Ti
Stg. Na-Ca	26.7	10.0	9.3	3.9	4.4	0.1	28.0
Least alt.	24.8	2.8	1.9	0.6	1.0	0.4	82.6

dote veinlets with albite haloes and pervasive albite-altered rocks (Figure 4f) at Valley-Lornex and Highmont. North and east of Bethlehem, rare tourmaline veinlets, with and without haloes of K-feldspar or intense white mica, are overprinted by epidote veins with albite–white mica haloes (Figure 5h). Sodic-calcic–altered rocks are crosscut by prehnite veinlets with plagioclase-destructive white mica haloes (Figures 5c, d) but still have distinctive major- and minor-element enrichments and depletions: elevated Na_2O, CaO and Cl; a decrease in K_2O and FeO; and high Na/Ba and Sr/Ba (e.g., Figure 5e).

Discussion

The recognition and study of the Na-Ca alteration assemblage is important because

- mapping has shown that large domains of strongly Na-Ca–metasomatized rocks are along strike of the porphyry Cu centres (Figure 2b);
- it locally removed magnetite and hornblende, thus changing the rock petrophysical properties; and
- where it overprinted Cu mineralization, it is destructive of the Cu grade.

Isotope and fluid-inclusion studies have shown that meteoric (Sheets et al., 1996; Taylor, 1979; Selby et al., 2000), formational brine (Dilles et al., 1992) and magmatic-derived (Dilles et al., 1992; Harris et al., 2005; Rusk et al., 2008) fluids of varying salinities can all be present in various proportions at different locations and times in an evolving porphyry system. Additionally, sericite at Koloula and Waisoi in Papua New Guinea is interpreted to have formed from seawater in young (1.5–5 Ma) and shallowly emplaced porphyry systems (Chivas et al., 1984). Similarly, calculated initial O and D isotopic compositions of coarse muscovite from the Valley system at HVC suggest mixing of seawater with high-temperature (370–500°C), Cu-bearing magmatic fluids (Osatenko and Jones, 1976).

Widespread Na-Ca alteration may be caused by the flow of external hypersaline formation waters, heated during inflow to the magmatic cupola regions along the margins of potassic alteration (Dilles et al., 1992; Dilles et al., 2000). Highly oxidized felsic magmas can produce fluids capable of Na-, Fe-, Ca- or K-rich alteration (Arancibia and Clark, 1996). Similarly, fluids evolved from special alkalic melts can cause Na metasomatism (Lang et al., 1995). The magmatic-derived Na-Ca–alteration examples, however, are inconsistent with the scale and distribution features of Na-Ca alteration in the Guichon batholith. Sodium-rich alteration is widely developed in Permian to Jurassic arc igneous rocks of the western United States, where it is attributed to moderate- to high-salinity fluids of marine, formation and/or meteoric origin, with or without a magmatic component (Battles and Barton, 1995). The hypothesis that will be tested in this study is that seawater drawn down and inward along regional structures toward cupola regions caused Na-Ca alteration during the upwelling of the magmatic-hydrothermal fluids that formed the porphyry Cu mineralization. If this is the case, this process may be more prevalent in island-arc porphyry systems than previously recognized.

This hypothesis will be tested using a combination of field and laboratory techniques. First, field maps, feldspar-stained rock slabs, hyperspectral images and petrography will be used to establish the Na-Ca facies distribution, mineralogy and its paragenesis at HVC. This will be followed by geochemical characterization by electron microprobe analysis (EMPA) and laser-ablation inductively coupled plasma–mass spectrometry (LA-ICP-MS) of the associated minerals (epidote, albite, actinolite, titanite). Results will be compared to Na, Ca and Na-Ca assemblages in other systems: Yerington, Anne-Mason and Royston in Nevada (Carten, 1986; Dilles and Einaudi, 1992); Sierrita-Esperanza and Kelvin-Riverside in Arizona (Seedorff et al., 2008); and Island Copper, Mt. Milligan, Gibraltar and Woodjam in BC (Arancibia and Clark, 1996; Jago et al., 2014; Chapman et al., 2015; Kobylinski et al., 2016). Whole-rock $^{87}Sr/^{86}Sr$ values of unaltered samples will be compared to the Sr-isotope composition of strongly Na-Ca–altered samples to test for shifts from initial HVC magmatic compositions of 0.7034 (D'Angelo, 2016) to Triassic seawater values of ~0.7076 (Tremba et al., 1975). Additionally, the Sr, O and D isotope compositions of epidote, albite and actinolite will be measured and evaluated with respect to magmatic and other fluid-reservoir (e.g., meteoric and seawater) compositions. Minerals formed from magmatic fluids are expected to have initial ä^{18}O and äD values close to 6‰ and –60‰, respectively (Taylor, 1979), whereas minerals formed from a fluid with seawater input may move toward the composition of standard mean ocean water (SMOW; ~0‰ for both ä^{18}O and äD).

◄

Figure 5. a) Epidote vein with albite halo in Skeena granodiorite crosscut by a quartz–K-feldspar–chalcopyrite veinlet. **b)** Feldspar-stained image of photo (a); dark yellow indicates K-feldspar and pink indicates calcic plagioclase; weak pink-stained to white plagioclase is associated with fine-grained, pale green, white mica and small grains of prehnite. **c)** and **d)** Epidote-quartz vein with K-feldspar–destructive albite halo crosscut, offset and overprinted by a prehnite veinlet with strong white mica–prehnite–chlorite halo; hostrock is Chataway-facies granodiorite. **e)** Irregular epidote veins with albite-chlorite haloes in Guichon granodiorite, also showing lithogeochemical response of the corresponding sample. **f)** Photomicrograph of albite- and white mica–altered feldspar and actinolite-epidote–altered hornblende in Guichon granodiorite; tourmaline vein fill is crosscut by epidote. **g)** Back-scattered electron image of partially actinolite-altered primary hornblende; note accessory titanite; primary feldspar is altered to albite and contains numerous disseminated inclusions of white mica and very fine grained pore space (black). **h)** Fragments of tourmaline in compositionally zoned (Fe-Al substitution) epidote. Mineral abbreviations: ab, albite; act, actinolite; ccp, chalcopyrite; chl, chlorite; ep, epidote; fsp, feldspar; hbl, hornblende; kfs, K-feldspar; pl, plagioclase; prh, prehnite; qz, quartz; ttn, titanite (sphene); tur, tourmaline; wm, white mica.

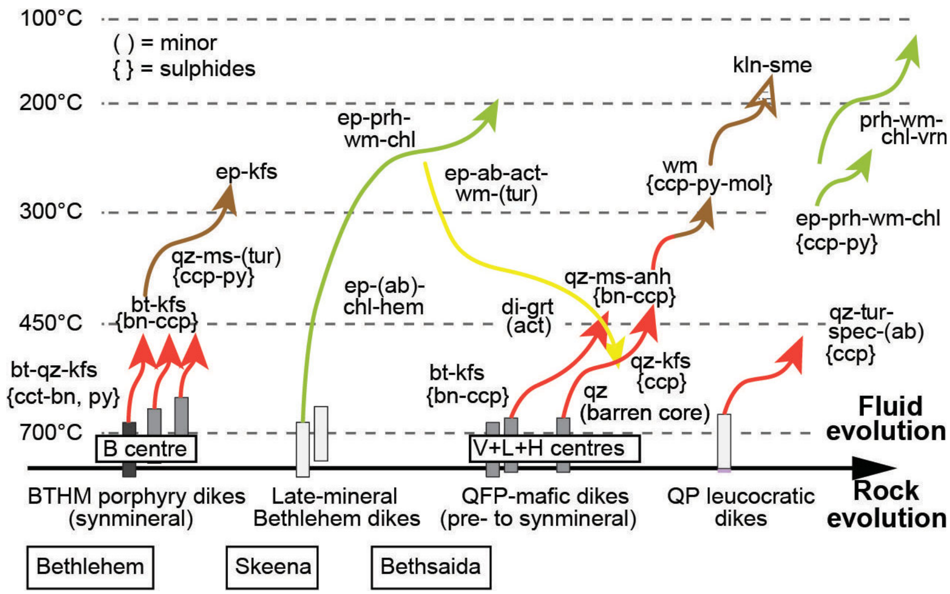

Figure 6. Paragenetic sequence of intrusion facies (rectangles) and vein and alteration facies (coloured arrows) at Highland Valley Copper (HVC). The colour scheme of the vein and alteration arrows is explained in Figure 3. The arrows are schematic representations of fluid evolution through time (x axis) and temperature changes (y axis). Abbreviations: B, Bethlehem; V, L and H, Valley, Lornex and Highmont, respectively. Mineral abbreviations: ab, albite; act, actinolite; anh, anhydrite; bn, bornite; bt, biotite; ccp, chalcopyrite; chl, chlorite; di, diopside; ep, epidote; grt, garnet; hem/spec, hematite; kln, kaolinite; kfs, K-feldspar; mol, molybdenite; ms, muscovite (coarse grained); prh, prehnite; py, pyrite; qz, quartz; sme, smectite; tur, tourmaline; vrm, vermiculite; wm, white mica–sericite (fine grained).

Impact of Proposed Work

Porphyry Cu deposits provide the world with most of its Cu and have likely been the focus of more academic research than any other class of base-metal deposit. Significant advances in genetic understanding of porphyry systems, at various scales, have been made. Exploration tools and models (e.g., Holliday and Cooke, 2007) applicable to the exploration geoscientist, however, have not advanced to the same degree, with a few notable exceptions: fertility (Richards, 2011a; Loucks, 2014); epidote-vector geochemistry (Jago, 2008; Cooke et al., 2014); lateral and vertical metal zonation (Jones, 1992; Halley et al., 2015); shortwave-infrared spectroscopy (Thompson et al., 1999; Halley et al., 2015); and porphyry-indicator minerals (Averill, 2011).

The research outlined in this paper is designed to test for evidence of nonmagmatic fluid flow around porphyry Cu deposits, and how these fluids interacted with and affected wallrock with increasing distance from the Cu centres. The nonconcentric distribution of Na-Ca alteration is an important modifier to typical alteration-zonation models. Results from this research have the potential to refine exploration models and leverage existing datasets, thus leading to more cost-efficient and successful exploration programs.

Acknowledgments

Funding was provided by the Natural Sciences and Engineering Council of Canada (NSERC) and the Canada Mining Innovation Council (CMIC) through the NSERC Collaborative Research and Development Program, for which the authors are grateful (NSERC-CMIC Exploration Footprints Network Contribution 115). Additionally, the authors thank the Strategic Planning Group at HVC and Teck Resources Limited for support during the summer fieldwork periods. This contribution benefited from review by L. Marshall, Regional Chief Geoscientist at Teck, and L. Pyrer.

References

Arancibia, O.N. and Clark, A. (1996): Early magnetite-amphibole-plagioclase alteration-mineralization in the Island Copper porphyry copper-gold-molybdenum deposit, British Columbia; Economic Geology, v. 91, p. 402–438.

Averill, S.A. (2011): Viable indicator minerals in surficial sediments for two major base metal deposit types: Ni-Cu-PGE and porphyry Cu; Geochemistry: Exploration, Environment, Analysis, v. 11, no. 4, p. 279–291. doi:10.1144/1467-7873/10-IM-022

Battles, D.A. and Barton, M.D. (1995): Arc-related sodic hydrothermal alteration in the western US; Geology, v. 23, no. 10, p. 913–916.

Byrne, K., Stock, E., Ryan, J., Johnson, C., Nisenson, J., Alva-Jimenez, T., Lapointe, M., Stewart, H., Grubisa, G. and Sykora, S. (2013): Porphyry Cu-(Mo) deposits in the Highland Valley District, South Central British Columbia; *in* Porphyry Systems of Central and Southern BC: Tour of Central BC Porphyry Deposits from Prince George to Princeton, J. Logan and T. Schroeter (ed.), Society of Economic Geologists, Guidebook Series, v. 44, p. 99–116, URL <http://www.segweb.org/store/detail.aspx?id=GB44-DISC> [November 2016].

Carten, R.B. (1986): Sodium-calcium metasomatism: chemical, temporal, and spatial relationships at the Yerington, Nevada porphyry copper deposit; Economic Geology, v. 81, no. 6, p. 1495–1519. doi:10.2113/gsecongeo.81.6.1495

Chapman, J., Plouffe, A. and Ferbey, T. (2015): Tourmaline chemistry as a tool for porphyry exploration: the Woodjam Cu-Au deposits, central British Columbia; Association for Mineral Exploration (AME) Roundup 2015, poster presentation.

Chivas, A.R., O'Neil, J.R. and Katchan, G. (1984): Uplift and submarine formation of some Melanesian porphyry copper deposits: stable isotope evidence; Earth and Planetary Science Letters, v. 68, p. 326–334.

Colpron, M., Nelson, J.A.L. and Murphy, D.C. (2007): Northern Cordilleran terranes and their interactions through time; GSA Today, v. 17, no. 4, p. 4–10. doi:10.1130/GSAT01704-5A.1

Coney, P.J., Jones, D.L. and Monger, J.W.H. (1980): Cordilleran suspect terranes; Nature, v. 288, p. 329–333.

Cooke, D.R., Baker, M., Hollings, P., Sweet, G., Zhaoshan, C., Danyushevsky, L., Gilbert, S., Zhou, T., White, N.C., Gemmell, J.B. and Inglis, S. (2014): New advances in detecting the distal geochemical footprints of porphyry systems: epidote mineral chemistry as a tool for vectoring and fertility assessments; *in* Building Exploration Capability for the 21st Century, K.D. Kelley and H.C. Golden (ed.), Society of Economic Geologists, Special Publication 18, p. 127–152.

D'Angelo, M. (2016): Geochemistry, petrography and mineral chemistry of the Guichon Creek and Nicola batholiths, south-central British Columbia; M.Sc. thesis, Lakehead University, Thunder Bay, Ontario, 435 p., URL <http://cmic-footprints.ca/home/publications/files/Theses/088_D%27Angelo_2016%20Lakehead%20MSc_Guichon%20Creek%20Batholith.pdf> [November 2016].

Dilles, J.H. and Einaudi, M.T. (1992): Wall-rock alteration and hydrothermal flow paths about the Ann-Mason porphyry copper deposit, Nevada: a 6-km vertical reconstruction; Economic Geology, v. 87, p. 1963–2001.

Dilles, J.H., Einaudi, M.T., Proffett, J.M. and Barton, M.D. (2000): Overview of the Yerington porphyry copper district: magmatic to nonmagmatic sources of hydrothermal fluids, their flow paths, alteration affects on rocks, and Cu-Mo-Fe-Au ores; Society of Economic Geologists, Post-Meeting Field Conference, v. 32, p. 55–66.

Dilles, J.H., Solomon, G.C., Taylor, H.P. and Einaudi, M.T. (1992): Oxygen and hydrogen isotope characteristics of hydrothermal alteration at the Ann-Mason porphyry copper deposit, Yerington, Nevada; Economic Geology, v. 87, no. 1, p. 44–63. doi:10.2113/gsecongeo.87.1.44

Halley, S.W., Dilles, J.H. and Tosdal, R.M. (2015): Footprints: hydrothermal alteration and geochemical dispersion around porphyry copper deposits; SEG Newsletter, no. 100.

Harris, A.C., Golding, S.D. and White, N.C. (2005): Bajo de la Alumbrera copper-gold deposit: stable isotope evidence for a porphyry-related hydrothermal system dominated by magmatic aqueous fluids; Economic Geology, v. 100, no. 5, p. 863–886. doi:10.2113/gsecongeo.100.5.863

Holliday, J.R. and Cooke, D.R. (2007): Advances in geological models and exploration methods for copper±gold porphyry deposits; *in* Proceedings of Exploration 07: Fifth Decennial International Conference on Mineral Exploration, p. 791–809.

Hollister, V.F., Allen, J.M., Anzalone, S.A. and Seraphim, R.H. (1976): Structural evolution of porphyry mineralization at Highland Valley, British Columbia: reply; Canadian Journal of Earth Sciences, v. 13, p. 612–613. doi:10.1139/e76-065

Jago, C.P. (2008): Metal- and alteration-zoning, and hydrothermal flow paths at the moderately-tilted, silica-saturated Mt. Milligan Cu-Au alkalic porphyry deposit; M.Sc. thesis, The University of British Columbia, Vancouver, BC, 227 p.

Jago, C., Tosdal, R., Cooke, D. and Harris, A. (2014): Vertical and lateral variation of mineralogy and chemistry in the Early Jurassic Mt. Milligan alkalic porphyry Au-Cu deposit, British Columbia, Canada; Economic Geology, v. 109, p. 1005–1033. doi:10.2113/econgeo.109.4.1005

Jones, B.K. (1992): Application of zoning to Au exploration in porphyry copper systems; Journal of Geochemical Exploration, v. 43, p. 127–155.

Kobylinski, C., Hattori, K., Smith, S. and Plouffe, A. (2016): Mineral chemistry of greenrock alteration associated with the porphyry Cu-Mo mineralization at the Gibraltar deposit, south central British Columbia, Canada; paper presented at Geological Association of Canada–Mineralogical Association of Canada, Joint Annual Meeting, Whitehorse, Yukon.

Lang, J., Stanley, C., Thompson, J.F.H. and Dunne, K. (1995): Na-K-Ca magmatic-hydrothermal alteration in alkalic porphyry Cu-Au deposits, British Columbia; *in* Magmas, Fluids and Ore Deposits, J.F.H. Thompson (ed.), Mineralogical Association of Canada, p. 339–366.

Lesage, G., Byrne, K., Lypaczewski, P., Lee, R.G. and Hart, C.J.R. (2016): Characterizing the district-scale alteration surrounding a large porphyry Cu system: the footprint of Highland Valley Copper, British Columbia; paper presented at Geological Association of Canada–Mineralogical Association of Canada, Joint Annual Meeting, Whitehorse, Yukon, <http://cmic-footprints.ca/home/publications/files/Posters/Lesage_2016 GAC MAC_HVC alteration_Poster.pdf> [November 2016].

Logan, J.M., and Mihalynuk, M.G. (2014): Tectonic controls on early Mesozoic paired alkaline porphyry deposit belts (Cu-Au±Ag-Pt-Pd-Mo) within the Canadian Cordillera; Economic Geology, v. 109, no. 4, p. 827–858. doi:10.2113/econgeo.109.4.827

Loucks, R.R. (2014): Distinctive composition of copper-ore-forming arc magmas; Australian Journal of Earth Sciences, v. 61, no. 1, p. 5–16. doi: 10.1080/08120099.2013.865676

Massey, N.W.D., MacIntyre, D.G., Desjardins, P. and Cooney, R.T. (2005): Digital geology map of British Columbia – whole province; BC Ministry of Energy and Mines, BC Geological Survey, GeoFile 2005-1, <http://www.empr.gov.bc.ca/Mining/Geoscience/PublicationsCatalogue/GeoFiles/Pages/2005-1.aspx> [December 2016].

McMillan, W.J. (1976): Geology and genesis of the Highland Valley ore deposits and the Guichon Creek Batholith; *in* Porphyry Deposits of the Canadian Cordillera, A. Sutherland Brown (ed.), Canadian Institute of Mining and Metallurgy, Special Volume 15, p. 85–104.

McMillan, W.J. (1985): Geology and ore deposits of the Highland Valley camp; Geological Association of Canada, Mineral Deposits Division, Field Guide and Reference Manual Series (A.J. Sinclair, ser. ed.), no. 1, 121 p.

McMillan, W.J., Anderson, R.G., Chen, R. and Chen, W. (2009): Geology and mineral occurrences (MINFILE), the Guichon Creek Batholith and Highland Valley porphyry copper district, British Columbia; Geological Survey of Canada, Open File 6079, 3 maps. doi:10.4095/248060

Mihalynuk, M.G., Diakow, L.J., Friedman, R.M. and Logan, J.M. (2016): Chronology of southern Nicola arc stratigraphy and deformation; *in* Geological Fieldwork 2015, BC Ministry of Energy and Mines, BC Geological Survey, Paper 2016-1, p. 31–63.

Mortimer, N. (1987): The Nicola Group: Late Triassic and Early Jurassic subduction related volcanism in British Columbia; Canadian Journal of Earth Sciences, v. 24, p. 2521–2536.

Northcote, K.E. (1969): Geology and geochronology of the Guichon Creek Batholith; BC Ministry of Energy and Mines, Bulletin 56, 77 p.

Osatenko, M.J. and Jones, M.B. (1976): Valley Copper; *in* Porphyry Deposits of the Canadian Cordillera, A. Sutherland Brown (ed.), Canada Institute of Mining and Metallurgy, Special Volume 15, p. 130–143.

Preto, V.A. (1979): Geology of the Nicola Group between Merritt and Princeton; BC Ministry of Energy and Mines, Bulletin 69, 100 p.

Proffett, J.M. (2009): High Cu grades in porphyry Cu deposits and their relationship to emplacement depth of magmatic sources; Geology, v. 37, no. 8, p. 675–678. doi:10.1130/G30072A.1

Ray, G.E., Dawson, G.L. and Webster, I.C. (1996): The stratigraphy of the Nicola Group in the Hedley district, British Columbia, and the chemistry of its intrusions and Au skarns; Canadian Journal of Earth Sciences, v. 33, p. 1105–1126.

Richards, J.P. (2011a): High Sr/Y arc magmas and porphyry Cu±Mo±Au deposits: just add water; Economic Geology, v. 106, no. 7, p. 1075–1081.

Richards, J.P. (2011b): Magmatic to hydrothermal metal fluxes in convergent and collided margins; Ore Geology Reviews, v. 40, no. 1, p. 1–26.

Riedell, K.B. and Proffett, J.M. (2014): Batholithic and early halo type Cu-Mo deposits; Geological Society of America, 2014 Annual Meeting, paper 247-4, <https://gsa.confex.com/gsa/2014AM/webprogram/Handout/Paper245644/Bath and EHT deposits_Riedell-Proffett_300dpi_revd-141027.pdf> [November 2016].

Rusk, B.G., Reed, M.H. and Dilles, J.H. (2008): Fluid inclusion evidence for magmatic-hydrothermal fluid evolution in the porphyry copper-molybdenum deposit at Butte, Montana; Economic Geology, v. 103, no. 2, p. 307–334. doi:10.2113/gsecongeo.103.2.307

Schodde, R. (2014): The global shift to undercover exploration: how fast? how effective?; presentation at Society of Economic Geologists, 2014 Annual Meeting, Keystone, Colorado, September 30, 2014.

Seedorff, E., Barton, M.D., Stavast, W.J. and Maher, David, J. (2008): Root zones of porphyry systems: extending the porphyry model to depth; Economic Geology, v. 103, p. 939–956.

Seedorff, E., Dilles, J.H., Proffett, J.M., Einaudi, M.T., Zurcher, L., Stavast, W.J.A., Johnson, D.A. and Barton, M.D. (2005): Porphyry deposits: characteristics and origin of hypogene features; *in* Economic Geology 100th Anniversary Volume, J. Hedenquist, J.F. Thompson, R. Goldfarb and J. Richards (ed.), Society of Economic Geologists, p. 251–298.

Selby, D., Nesbitt, B.E., Muehlenbachs, K. and Prochaska, W. (2000): Hydrothermal alteration and fluid chemistry of the Endako porphyry molybdenum deposit, British Columbia; Economic Geology, v. 95, no. 1, p. 183–202.

Sheets, R.W., Nesbitt, B.E. and Muehlenbachs, K. (1996): Meteoric water component in magmatic fluids from porphyry copper mineralization, Babine Lake area, British Columbia; Geology, v. 24, no. 12, p. 1091–1094.

Sillitoe, R.H. (2010): Porphyry copper systems; Economic Geology, v. 105, no. 1, p. 3–41. doi:10.2113/gsecongeo.105.1.3

Sillitoe, R.H. (2013): Metallogenic and regulatory inequalities around the northern Pacific Rim: implications for discovery; *in* Tectonics, Metallogeny, and Discovery: The North American Cordillera and Similar Accretionary Settings, M. Colpron, T. Bissig, B.G. Rusk and J.F.H. Thompson (ed.), Special Publication 17, p. 1–16.

Taylor, H.P. (1979): Oxygen and hydrogen isotope relationships in hydrothermal mineral deposits; *in* Geochemistry of Hydrothermal Ore Deposits, H.L. Barnes (ed.), John Wiley & Sons, New York, New York, p. 236–277.

Teck Resources Limited (2016): Annual information form, 117 p., <http://www.teck.com/media/Investors-aif_march_2016_T5.1.2.pdf> [November 2016].

Thompson, A.J.B., Hauf, P.L. and Robitaille, A.J. (1999): Alteration mapping in exploration: applications of short-wave infrared (SWIR) spectroscopy; SEG Newsletter, no. 39, p. 13.

Thompson, J.F.H. (2016): The future of mineral exploration; presentation at Association for Mineral Exploration (AME) Roundup 2016, Vancouver, BC.

Tremba, E.L., Faure, G., Katsikatsos, G.C. and Summerson, C.H. (1975): Strontium isotope composition in the Tethys Sea, Euboea, Greece; Chemical Geology, v. 16, p. 109–120.

Wilburn, D.R., Stanley, K.A. and Karl, N.A. (2015): Exploration review; Mining Engineering, Annual Review 2014, v. 67, no. 5, p. 16–38. <http://me.smenet.org/abstract.cfm?preview=1&articleID=5905&page=16> [December 2016].

Wood, D. (2016): We must change exploration thinking in order to discover future orebodies; SEG Newsletter, no. 105, p. 16–19.